PROCEEDINGS OF SCIENCE

Measurement of $BR(K \to e\nu)/BR(K \to \mu\nu)$ in NA62

Antonino Sergi[*†]
CERN
E-mail: antonino.sergi@cern.ch

Measurement of the helicity suppressed ratio of charged kaon leptonic decay rates $BR(K \to e\nu)/BR(K \to \mu\nu)$ has long been considered as an excellent test of lepton universality and the Standard Model (SM) description of weak interactions. It was realized recently that the suppression of the SM contribution might enhance the sensitivity to SUSY-induced effects to an experimentally accessible level. The NA62 experiment at the CERN SPS has collected a record number of over 10^5 $K \to e\nu$ decays during a dedicated run in 2007, aiming at achieving 0.5% precision. Experimental strategy, details of the analysis and preliminary results are discussed.

The Xth Nicola Cabibbo International Conference on Heavy Quarks and Leptons,
October 11-15, 2010
Frascati (Rome) Italy

[*]Speaker.
[†]On behalf of NA62 Collaboration.

PoS(HQL 2010)026

1. Introduction

Decays of pseudoscalar mesons to light leptons are suppressed in the Standard Model (SM) by angular momentum conservation. In particular, the SM width of $P^{\pm} \to l^{\pm}\nu$ decays (with $P = \pi, K, D_{(s)}, B$) is

$$\Gamma^{\rm SM} = \frac{G_F^2 M_P M_\ell^2}{8\pi}\left(1-\frac{M_\ell^2}{M_P^2}\right)^2 f_P^2 |V_{qq'}|^2,$$

where G_F is the Fermi constant, M_P and M_ℓ are meson and lepton masses, f_P is the decay constant, and $V_{qq'}$ is the corresponding CKM matrix element.

Within the two Higgs doublet models (2HDM of type II), including the minimal supersymmetric one, the charged Higgs boson ($H^{\pm}$) exchange induces a tree-level contribution to (semi)leptonic decays proportional to the Yukawa couplings of quarks and leptons [1]. In $P^{\pm} \to \ell^{\pm}\nu$, it can compete with the $W^{\pm}$ exchange due to the helicity suppression of the latter. At tree level, the $H^{\pm}$ exchange contribution is lepton flavour independent, and for $P = \pi, K, B$ leads to [2]

$$\frac{\Gamma(P^{\pm} \to \ell^{\pm}\nu)}{\Gamma^{\rm SM}(P^{\pm} \to \ell^{\pm}\nu)} = \left[1-\left(\frac{M_P}{M_H}\right)^2 \frac{\tan^2\beta}{1+\varepsilon_0\tan\beta}\right]^2.$$

Here M_H is the $H^{\pm}$ mass, $\tan\beta$ is the ratio of the two Higgs vacuum expectation values, and $\varepsilon_0 \approx 10^{-2}$ is an effective coupling.

A plausible choice of parameters $M_H = 500$ GeV$/c^2$, $\tan\beta = 40$ leads to $\sim 30\%$ relative suppression of $B^+ \to \ell^+\nu$ decays, and $\sim 0.3\%$ suppression of $K^+, D_s^+ \to \ell^+\nu$ decays with respect to their SM rates. However, searches for new physics in the decay rates are hindered by the uncertainties of their SM predictions. On the other hand, the ratio of kaon leptonic decay widths $R_K = \Gamma(K_{e2})/\Gamma(K_{\mu 2})$, where the notation $K_{\ell 2}$ is adopted for $K^+ \to \ell^+\nu$ decays, is sensitive to loop-induced lepton flavour violating (LFV) effects via the $H^{\pm}$ exchange [3]:

$$\Delta R_K / R_K^{\rm SM} \simeq \left(\frac{M_K}{M_H}\right)^4 \left(\frac{M_\tau}{M_e}\right)^2 |\Delta_R^{31}|^2 \tan^6\beta,$$

where the mixing parameter between the superpartners of the right-handed leptons $|\Delta_R^{31}|$ can reach $\sim 10^{-3}$. This can enhance R_K by $\mathcal{O}(1\%)$ relative without contradicting any presently known experimental constraints, including upper bounds on the LFV decays $\tau \to eX$ with $X = \eta, \gamma, \mu\mu$.

Unlike the individual $K_{\ell 2}$ decay widths, the ratio $R_K = \Gamma(K_{e2})/\Gamma(K_{\mu 2})$ is precisely predicted within the SM due to cancellation of hadronic uncertainties [4]:

$$R_K^{\rm SM} = \left(\frac{M_e}{M_\mu}\right)^2 \left(\frac{M_K^2 - M_e^2}{M_K^2 - M_\mu^2}\right)^2 (1+\delta R_{\rm QED}) = (2.477 \pm 0.001) \times 10^{-5},$$

where $\delta R_{\rm QED} = (-3.79 \pm 0.04)\%$ is an electromagnetic correction due to the internal bremsstrahlung (IB) process.

The sensitivity to LFV and the precision of the SM prediction make R_K an excellent probe of lepton universality. The current world average (based on final results only) $R_K^{\rm WA} = (2.490 \pm 0.030) \times 10^{-5}$ is dominated by a recent KLOE result [5]. A precise measurement of R_K based on a part (40%) of the data sample collected by the CERN NA62 experiment in 2007 is reported here. This is an update of an earlier result obtained with the same data sample [6].

2. Experimental Setup

The NA48/2 experimental setup [7] has been used for the NA62 2007–08 data taking. Experimental conditions have been optimized for the $K_{e2}/K_{\mu 2}$ measurement. Although the beam line is designed to deliver simultaneous unseparated K^+ and K^- beams derived from the SPS 400 GeV/c primary protons, the sample used for the present analysis was collected with the K^+ beam only. Positively charged particles within a momentum band of (74.0 ± 1.6) GeV/c are selected by an achromatic system of four dipole magnets with zero total deflection, pass through a muon sweeping system, and enter a fiducial decay volume contained in a 114 m long cylindrical vacuum tank with transverse size of $\delta x = \delta y = 7$ mm (rms) and negligible angular divergence.

The main detectors used for the measurement are a plastic scintillator hodoscope (HOD), for fast trigger and timing, a magnetic spectrometer, composed of four drift chambers (DCHs) and a dipole magnet, and a liquid krypton electromagnetic calorimeter (LKr), used for particle identification and as a veto, being almost homogeneous and $27X_0$ deep.

A minimum bias trigger configuration has been employed. The K_{e2} trigger condition consists of coincidence of hits in the two HOD planes (the Q_1 signal), loose lower and upper limits on DCH hit multiplicity (the 1-track signal), and LKr energy deposit ($E_{\rm LKr}$) of at least 10 GeV. The $K_{\mu 2}$ trigger condition requires a coincidence of the Q_1 and 1-track signals downscaled by a factor $D = 150$.

3. Measurement Strategy

The measurement strategy exploits the similar experimental signatures of K_{e2} and $K_{\mu 2}$, collecting them simultaneously thus neglecting the absolute flux and relying on first order cancellation of several systematic effects.

The ratio R_K in each bin is computed as

$$R_K = \frac{1}{D} \cdot \frac{N(K_{e2}) - N_{\rm B}(K_{e2})}{N(K_{\mu 2}) - N_{\rm B}(K_{\mu 2})} \cdot \frac{A(K_{\mu 2})}{A(K_{e2})} \cdot \frac{f_\mu \times \varepsilon(K_{\mu 2})}{f_e \times \varepsilon(K_{e2})} \cdot \frac{1}{f_{\rm LKr}},$$

where $N(K_{\ell 2})$ is the number of selected $K_{\ell 2}$ candidates ($\ell = e, \mu$), $N_{\rm B}(K_{\ell 2})$ is the number of background events, $A(K_{\mu 2})/A(K_{e2})$ is the geometric acceptance correction, f_ℓ is the lepton identification efficiency, $\varepsilon(K_{\ell 2})$ is the trigger efficiency, $f_{\rm LKr}$ is the global efficiency of the LKr readout, and $D = 150$ is the $K_{\mu 2}$ trigger downscaling factor. The measurement is performed in 10 bins of lepton momentum, between 13 and 65 GeV/c, independently optimizing the selection for each bin.

Acceptance corrections, both for signal and backgrounds, are evaluated by a detailed Monte Carlo (MC) simulation, while particle identification, trigger and readout efficiencies are measured directly from data.

Due to the topological similarity of K_{e2} and $K_{\mu 2}$ decays, a large part of the selection is common for the two modes: (1) exactly one reconstructed particle of positive electric charge geometrically consistent with originating from a kaon decay is required; (2) extrapolated track impact points in the DCHs, HOD and LKr must be within their geometrical acceptances; (3) track momentum must be in the range 13-65 GeV/c, where the lower limit assures the efficiency of the $E_{\rm LKr} > 10$ GeV trigger condition; (4) no LKr energy deposition clusters with energy $E > E_{\rm veto} = 2$ GeV and in time

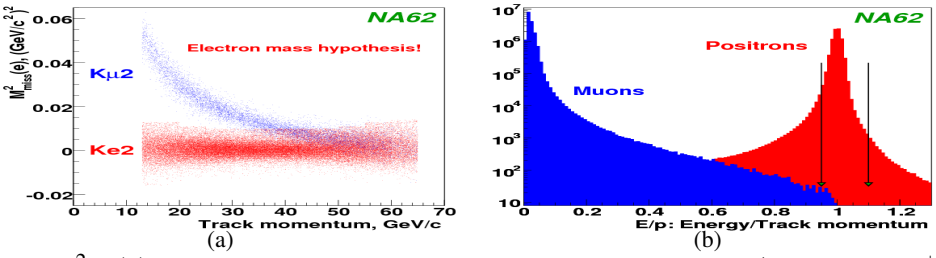

Figure 1: (a) $M^2_{\rm miss}(e)$ vs lepton momentum for K_{e2} and $K_{\mu 2}$ decays; (b) E/p spectra of e^+ and μ^+.

with the track are allowed unless they are consistent with being produced by the track via direct energy deposition or bremsstrahlung; (5) the reconstructed decay vertex longitudinal position must be within the nominal decay volume; (6) distance between the charged track and the nominal kaon beam axis must be below 3.5 cm.

The following two principal criteria are used to distinguish K_{e2} from $K_{\mu 2}$ decays. Kinematic identification is based on constraining the reconstructed squared missing mass in positron (muon) hypothesis $-M_1^2 < M^2_{\rm miss}(\ell) = (P_K - P_\ell)^2 < M_2^2$, where P_K and P_ℓ are the four-momenta of the kaon (defined as the average one monitored with $K^+ \to \pi^+\pi^+\pi^-$ decays) and the lepton (under the e^+ or μ^+ mass hypothesis). The limits M_1^2 and M_2^2 have been optimized taking into account the resolution and backgrounds, and vary among lepton momentum bins in the ranges 0.013-0.016 and 0.010-0.014 (GeV/c^2)^2, respectively. Lepton identification is based on the ratio E/p of track energy deposition in the LKr to its momentum measured by the spectrometer. Tracks with $(E/p)_{\rm min} < E/p < 1.1$, where $(E/p)_{\rm min} = 0.95$ for $p > 25$ GeV/c and $(E/p)_{\rm min} = 0.9$ otherwise, are identified as positrons. Tracks with $E/p < 0.85$ are identified as muons.

4. Backgrounds

Kinematic separation of K_{e2} from $K_{\mu 2}$ decays is achievable at low lepton momentum only ($p < 30$ GeV/c), as shown in Fig. 1a. At high lepton momentum, the $K_{\mu 2}$ decay with the muon mis-identified as positron ($E/p > 0.95$, as shown in Fig. 1b) due to 'catastrophic' bremsstrahlung, i.e. energy loss close to total energy, in or in front of the LKr is the largest background source. In order to measure the mis-identification probability $P_{\mu e}$, a muon sample free from the typical $\sim 10^{-4}$ positron contamination due to $\mu \to e$ decays has been collected: a $9.2X_0$ thick lead (Pb) wall covering $\sim 20\%$ of the geometric acceptance was installed in front of the LKr during a period of data taking. The Pb wall itself introduces a bias for this measurement, decreasing $P_{\mu e}$ at low momentum due to ionization in Pb and increasing it at high momentum due to bremsstrahlung; a correction factor $f_{\rm Pb} = P_{\mu e}/P^{\rm Pb}_{\mu e}$ has been evaluated by means of a dedicated Geant4 based [8] MC simulation, including muon bremsstrahlung [9]. Although the resulting uncertainty on $P^{\rm Pb}_{\mu e}$ is 10% (Fig. 2), $\delta f_{\rm Pb}/f_{\rm Pb} = 2\%$.

The $K_{\mu 2}$ background contamination has been computed to be $(6.10 \pm 0.22)\%$ using the measured $P^{\rm Pb}_{\mu e}$ corrected by the simulated $f_{\rm Pb}$, and correcting for the correlation between the reconstructed $M^2_{\rm miss}(e)$ and E/p. The uncertainty is due to the limited data sample used to measure $P^{\rm Pb}_{\mu e}$ (0.16%), $\delta f_{\rm Pb}$ (0.12%), and model-dependence of the $M^2_{\rm miss}(e)$ vs E/p correlation (0.08%).

The $K_{\mu 2}$ decay also contributes to background via the $\mu \to e$ decay in flight. Energetic forward daughter positrons compatible with K_{e2} kinematics and topology are suppressed by muon polariza-

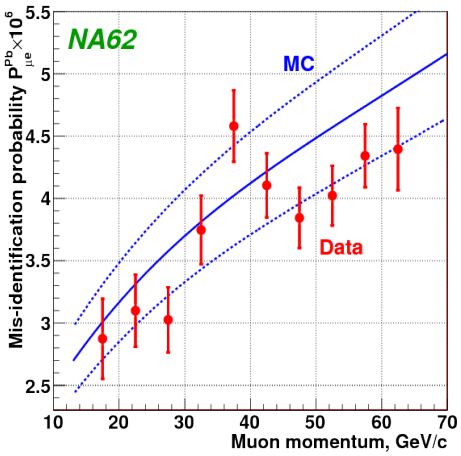

Figure 2: Muon mis-identification probability $P_{\mu e}^{\rm Pb}$ for $(E/p)_{\rm min} = 0.95$ vs momentum: measurement (markers with error bars); simulation with its uncertainty (solid and dashed lines).

tion effects [10]. Radiative corrections to the muon decay [11] lead to a further $\sim 10\%$ relative background suppression. The background contamination has been estimated to be $(0.27 \pm 0.04)\%$.

The structure-dependent (SD) $K^+ \to e^+\nu\gamma$ process [12], not suppressed by angular momentum conservation (more specifically, its SD^+ component corresponding to positive photon helicity), represents a significant background source. A recent measurement of the $K^+ \to e^+\nu\gamma$ (SD^+) differential decay rate [5] has been used to evaluate the background contamination to be $(1.15 \pm 0.17)\%$. The dominant uncertainty comes from the uncertainty on the rate of $K^+ \to e^+\nu\gamma$ (SD^+) decay, which has been increased by a factor of 3 with respect to that reported in [5], as suggested by a stability check of R_K with respect to a variation of the $E_{\rm veto}$ limit.

The beam halo background is induced by halo muons undergoing $\mu \to e$ decays in the vacuum tank, or being mis-identified as positrons. It has been measured directly by reconstructing the K_{e2}^+ candidates from a K^- data sample collected with the K^+ beam (but not its halo) blocked, and a special data sample collected with both beams blocked. The control sample is normalized to the data in the region $-0.3 < M^2_{\rm miss}(\mu) < -0.1$ $(\mathrm{GeV}/c^2)^2$ populated predominantly by beam halo events. The 'cross-talk' probability to reconstruct a K_{e2}^+ candidate due to a K^- decay with e^+ emission ($K^- \to \pi_D^0\ell^-\nu$, $K^- \to \pi^-\pi_D^0$, $K^- \to \ell^-\nu e^+e^-$, where π_D^0 denotes the π^0 Dalitz decay $\pi^0 \to \gamma e^+e^-$) is at the level of $\sim 10^{-4}$ and is taken into account. The halo background contamination has been estimated to be $(1.14 \pm 0.06)\%$, where the uncertainty comes from the limited size of the control sample and the uncertainty of its normalization. The beam halo is the only significant background source in the $K_{\mu 2}$ sample, measured to be $(0.38 \pm 0.01)\%$ with the same technique.

The number of $K_{\ell 2}$ candidates is $N(K_{e2}) = 59,963$ (about four times the statistics collected by KLOE) and $N(K_{\mu 2}) = 1.803 \times 10^7$. The $M^2_{\rm miss}(e)$ distributions of data events and backgrounds are presented in Fig. 3; backgrounds in the K_{e2} sample integrated over lepton momentum are summarized in Table 1.

5. Systematic Uncertainties

The ratio of geometric acceptances $A(K_{\mu 2})/A(K_{e2})$ in each lepton momentum bin has been evaluated with a MC simulation. The radiative $K^+ \to e^+\nu\gamma$ (IB) process is simulated follow-

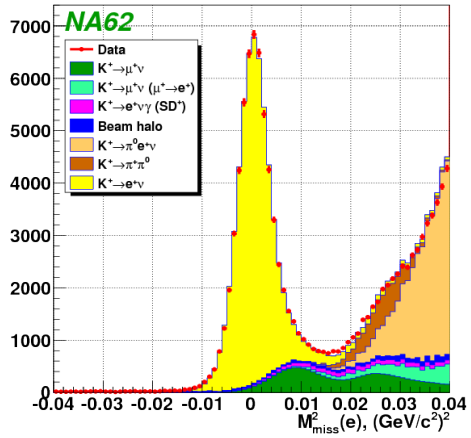

Figure 3: Reconstructed $M^2_{\rm miss}(e)$ distribution of the K_{e2} candidates and background components.

Source	$N_B/N(K_{e2})$
$K_{\mu 2}$	$(6.10 \pm 0.22)\%$
$K_{\mu 2}$ $(\mu \to e)$	$(0.27 \pm 0.04)\%$
$K_{e2\gamma}$ (SD^+)	$(1.15 \pm 0.17)\%$
Beam halo	$(1.14 \pm 0.06)\%$
K_{e3}	$(0.06 \pm 0.01)\%$
$K_{2\pi}$	$(0.06 \pm 0.01)\%$
Total background	$(8.78 \pm 0.29)\%$

Table 1: Summary of backgrounds in the K_{e2} sample.

ing [12] with higher order corrections according to [13, 14]. Lepton tracking inefficiency due to interactions with the spectrometer material is included into the acceptance correction, and its simulation has been validated with the data. The main sources of systematic uncertainty of the acceptance correction are the limited knowledge of beam profile and divergence, accidental activity, and the simulation of soft radiative photons. A separate uncertainty has been assigned due to the limited precision of the DCH alignment.

A sample of $\sim 4 \times 10^7$ positrons selected kinematically from $K^+ \to \pi^0 e^+ \nu$ decays collected concurrently with the main $K_{\ell 2}$ data set is used to calibrate the energy response of each LKr cell, and to study f_e with respect to local position and time stability (in the kinematically limited momentum range $p < 50$ GeV/c). A sample of electrons and positrons from the 4×10^6 $K_L \to \pi^\pm e^\mp \nu$ decays collected during a special short (15h) run with a broad momentum band K^0_L beam allows the determination of f_e in the whole analysis momentum range. The measurements of f_e have been performed in bins of lepton momentum. The inefficiency averaged over the K_{e2} sample is $1 - f_e = (0.73 \pm 0.05)\%$, where the uncertainty takes into account the statistical precision and the small differences between K^+ and K^0_L measurements.

The inefficiency of the Q_1 trigger condition has been measured using $K_{\mu 2}$ events triggered with a special control LKr signal: integrated over the $K_{\mu 2}$ sample, it is $(1.4 \pm 0.1)\%$. Owing to its geometric uniformity, and the similarity of the K_{e2} and $K_{\mu 2}$ distributions over the HOD plane, it mostly cancels between the K_{e2} and $K_{\mu 2}$ samples, and the residual systematic bias on R_K is negligible. The inefficiency of the 1-track trigger for $K_{\ell 2}$ modes is negligible. The trigger efficiency correction $\varepsilon(K_{\mu 2})/\varepsilon(K_{e2})$ is determined by the efficiency $\varepsilon(E_{\rm LKr})$ of the LKr energy deposit trigger signal $E_{\rm LKr} > 10$ GeV, which has been measured to be $1 - \varepsilon(E_{\rm LKr}) = (0.41 \pm 0.05)\%$ in the first lepton momentum bin of 13-20 GeV/c, and to be negligible in the other momentum bins. The corresponding uncertainty on R_K is negligible.

The 1-track trigger condition may be affected by energetic photons initiating showers in the DCH or beam pipe material, suppressing the $K^+ \to e^+ \nu\gamma$ (SD^+) background by about 10% relative (varying over the positron momentum). Evaluation of the 1-track inefficiency for $K^+ \to e^+ \nu\gamma$ (SD^+) partially relies on simulation; its uncertainty has been propagated into R_K.

The global LKr readout inefficiency has been measured using an independent readout system

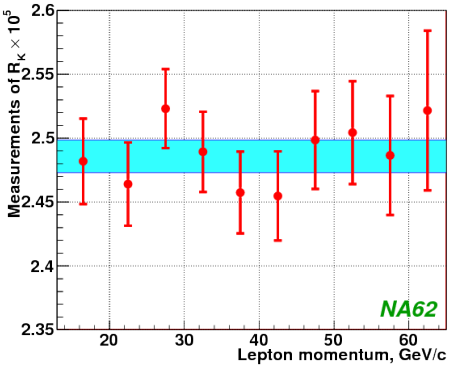

Figure 4: Measurements of R_K in lepton momentum bins, and the averaged R_K (band).

Source	$\delta R_K \times 10^5$
Statistical	0.011
$K_{\mu 2}$ background	0.005
$K^+ \to e^+ \nu\gamma$ (SD$^+$) background	0.004
Beam halo background	0.001
Acceptance correction	0.002
Spectrometer alignment	0.001
Positron identification	0.001
1-track trigger efficiency	0.002

Table 2: Summary of the uncertainties on R_K.

to be $1 - f_{\rm LKr} = (0.20 \pm 0.03)\%$ and stable in time.

6. Result And Conclusions

The independent measurements of R_K in the 10 lepton momentum bins and the average over the bins are displayed in Fig. 4. Extensive stability checks in bins of kinematic variables, against variation of selection criteria and analysis procedures have been performed. The uncertainties of the combined result are summarized in Table 2. The result is

$$R_K = (2.486 \pm 0.011_{\rm stat.} \pm 0.007_{\rm syst.}) \times 10^{-5} = (2.486 \pm 0.013) \times 10^{-5}.$$

This is the most precise measurement to date; it is consistent with the SM expectation.

References

[1] W.-S. Hou, Phys. Rev. D48 (1993) 2342.
[2] G. Isidori and P. Paradisi, Phys. Lett. B639 (2006) 499.
[3] A. Masiero, P. Paradisi and R. Petronzio, Phys. Rev. D74 (2006) 011701.
[4] V. Cirigliano and I. Rosell, Phys. Rev. Lett. 99 (2007) 231801.
[5] F. Ambrosino *et al.*, Eur. Phys. J. C64 (2009) 627. Erratum-ibid. C65 (2010) 703.
[6] E. Goudzovski, arXiv:1005.1192.
[7] V. Fanti *et al.*, Nucl. Instrum. Methods A574 (2007) 433.
[8] S. Agostinelli *et al.*, Nucl. Instrum. Methods A506 (2003) 250.
[9] S.R. Kelner, R.P. Kokoulin and A.A. Petrukhin, Phys. Atom. Nucl. 60 (1997) 576.
[10] L. Michel, Proc. Phys. Soc. A63 (1950) 514.
[11] A. Arbuzov, A. Czarnecki and A. Gaponenko, Phys. Rev. D65 (2002) 113006.
[12] J. Bijnens, G. Ecker and J. Gasser, Nucl. Phys. B396 (1993) 81.
[13] S. Weinberg, Phys. Rev. 140 (1965) B516.
[14] C. Gatti, Eur. Phys. J. C45 (2006) 417.